Langmuir
Article

pubs.acs.org/Langmuir

Eletrowetting Effect in a Nanoporous Silica

Weiyi Lu,[†] Taewan Kim,[‡] Aijie Han,[§] Xi Chen,[⊥] and Yu Qiao*[,†,‡]

[†]*Department of Structural Engineering, University of California−San Diego, San Diego, California 92093-0085,* [‡]*Program of Materials Science and Engineering, University of California−San Diego, San Diego, California 92093,* [§]*Department of Chemistry, University of Texas−Pam America, Edinburg, Texas 78539, and* [⊥]*Fu Foundation School of Engineering and Applied Science, Columbia University, New York, New York 10027*

Received February 24, 2009. Revised Manuscript Received May 7, 2009

In the past, electrowetting was usually analyzed on large solid surfaces. In the current study, the effective solid−liquid interfacial tension in a nanoporous silica, which is measured by the ion transport pressure, is investigated experimentally. The interfacial tension decreases as the applied potential difference increases, while the magnitude of variation is much smaller than its bulk counterpart. The effect of the external electric field is saturated at a relatively low voltage. These unique phenomena can be attributed to the confinement effect of nanopore walls.

I. Introduction

As a potential difference is generated across a solid-electrolyte interface, the system free energy can be changed considerably, which in turn affects the surface wettability.[1] Very often, electrowetting measurement is performed at the surface of a large, nonconductive flat layer, which separates a drop of electrolyte solution from an electrode.[2] The thickness of the nonconductive surface layer is typically in the range of a few micrometers to a fraction of a millimeter.[3,4] By applying a voltage between the electrode and the liquid, the contact angle can be adjusted in a wide range.[5,6] According to the classic electrochemistry theory, $\gamma = \gamma_1 - C\phi^2/2$, where γ is the interfacial tension, γ_1 is the reference wettability, C is the interfacial capacity, and ϕ is the applied potential difference. Note that, no matter whether the applied voltage is positive or negative, the interfacial tension always decreases as the magnitude of ϕ increases. The effective interfacial tension, γ, can be taken as $\gamma_{sv} - \gamma_{sl}$, with γ_{sv} and γ_{sl} being the solid−vapor and solid−liquid interfacial energies, respectively.

For the past decade, electrowetting of nanostructured surfaces has been an active area of research. Many studies revealed important wetting and dewetting phenomena under external electric fields[7−10] and/or other forms of loadings.[11−14] These investigations were focused on the wettability of outer (nonconfining) surfaces of nanostructures. In a confining nanoenvironment, e.g., at inner surfaces of nanochannels, nanotubes, or nanopores, the electrowetting phenomena can be quite different. For instance, Prins et al. [15] developed a microtransport device by using a membrane containing straight microchannels. The inner surfaces of the microchannels were coated by insulation layers. As an external electric field was applied across the solid and the liquid phases, the wetting characteristics of the channel walls could be controlled quite precisely, which caused a surface tension-driven microfluidic motion. In this study, the microchannel size was at the level of 10^2 μm, and the variation of interfacial tension fitted well with the data of contact angle measurements. Other applications of electrowetting techniques include adjustment of liquid morphology,[16] nanomaterials processing,[17] and so forth.

Recently, using thermal or electrical methods to control nanofluidic behaviors has drawn increasing attention.[18,19] For example, a nanoporous material-functionalized (NMF) liquid can be formed by suspending hydrophobic nanoporous particles in a liquid phase. The nanopores can be filled only when a sufficiently high pressure is applied.[20−22] As the liquid molecules contact the nonwettable nanopore surfaces, the system free energy largely increases by $\gamma \cdot A_0$, with A_0 being the total surface area. In a number of systems, the confined liquid does not defiltrate when the external pressure is lowered, and thus the increase in system free energy is dissipated. The mechanical work is converted either to interfacial tension[23] or thermal energy.[24,25]

One of the key parameters that dominate the performance of NMF liquids is the transport pressure of the confined liquid,

*Corresponding author. Phone: 858-534-3388. Fax: 858-822-2260. E-mail: yqiao@ucsd.edu.

(1) Cho, S. K.; Moon, H. *Biochip J*. **2008**, *2*, 79–96.
(2) The, S. Y.; Lin, R; Hung, L. H.; Lee, A. P. *Lab Chip* **2008**, *8*, 198–220.
(3) Haeberle, S; Zengerle, R. *Lab Chip* **2007**, *7*, 1094–1110.
(4) Gras, S. L.; Mahmud, T; Rosengarten, G; Mitchell, A; Kalantar-Zadeh, K. *ChemPhysChem* **2007**, *8*, 2036–2050.
(5) Mugele, F; Baret, J. C. *J. Phys.: Condens. Matter* **2005**, *17*, R705–R774.
(6) Darhuber, A. A.; Troian, S. M. *Annu. Rev. Fluid Mech*. **2005**, *37*, 425–455.
(7) Verplanck, N.; Galopin, E.; Camart, J. C.; Thomy, V.; Coffinier, Y.; Boukherroub, R. *Nano Lett*. **2007**, *7*, 813.
(8) Brunet, P.; Lapierre, F.; Thomy, V.; Coffinier and, Y.; Boukherroub, R. *Langmuir* **2008**, *24*(19), 11203–11208.
(9) Bahadur Garimella, E. W. *Langmuir*, in press
(10) Staicu, A.; , Manukyan, G.; , Mugele, F.; . Microscopic structure of electrowetting-driven transitions on superhydrophobic surfaces available. arXiv: 0801.2683v1 [physics.flu-dyn].
(11) Bartolo, D.; Bouamrirene, F.; Verneuil, E.; Buguin, A.; Silberzan, P.; Moulinet, S. *Europhys. Lett*. **2006**, *74*(2), 299–305.
(12) Reyssat, M.; Pepin, A.; Marty, F.; Chen, Y.; Quere, D. *Europhys. Lett*. **2006**, *74*(2), 306–312.
(13) Lafuma, A.; Quéré, D. *Nat. Mater*. **2003**, *2*, 457–460.
(14) Bormashenko, E.; Pogreb, R.; Whyman, G.; Erlich, M. *Appl. Phys. Lett*. **2007**, *90*, 201917.
(15) Prins, M. W. J.; Welters, W. J. J.; Weekamp, J. W. *Science* **2001**, *291*, 277–280.
(16) Chang, C. C.; Yang, R. J. *Microfluid. Nanofluid*. **2007**, *3*, 501–525.
(17) Kim, D.; Lu, W. *Nanotechnology* **2004**, *15*, 667–674.
(18) Kong, X; Qiao, Y. *J. Appl. Phys*. **2006**, *99*, 064313.
(19) Han, A; Qiao, Y. *Appl. Phys. Lett*. **2007**, *91*, 173123.
(20) Punyamurtula, V. K.; Qiao, Y. *Mater. Res. Innovations* **2007**, *11*, 37–39.
(21) Punyamurtula, V. K.; Qiao, Y. *Microporous Mesoporous Mater*. **2007**, *103*, 35–39.
(22) Han, A; Qiao, Y. *J. Mater. Res*. **2007**, *22*, 3538–3541.
(23) Qiao, Y; Punyamurtula, V. K.; Xian, G; Karbhari, V. M.; Han, A. *Appl. Phys. Lett*. **2008**, *92*, 063109.
(24) Han, A; Punyamurtula, V. K.; Qiao, Y. *J. Mater. Res*. **2008**, *23*, 1902–1906.
(25) Han, A; Lu, W; Punyamurtula, V. K.; Kim, T; Qiao, Y. *J. Appl. Phys*. **2009**, *105*, 024309.

P_{in}, i.e., the critical pressure that overcomes the capillary effect of nanopore walls. In the past, a few techniques have been developed to control P_{in}, by adjusting the nanoprous structure,[26] surface treatment,[27−29] and/or using chemical admixtures.[30−33] However, if the system works in a changing environment, the value of P_{in} may vary over time, which can cause unexpected loss in energy dissipation capacity. For instance, it was noticed that, if temperature increases, P_{in} can be significantly decreased.[34] This softening effect must be taken into consideration for systems where stable performance is required in broad temperature ranges.

A possible environmental factor that can be employed to control P_{in} is the external electric field. However, the study on the electric field effect on solid−liquid interfacial tension in a confining nanoenvironment is still in its early stage. As suggested by a number of researchers,[35−38] many physical and chemical concepts, including the definitions of density, viscosity, and phase diagram of liquids, need to be reinvestigated at the nanometer scale, for which not only fundamental understanding but also basic testing data are still lacking. In a recent study[39] it was argued that, in a nanopore, the classic Laplace−Young equation is no longer valid. A new term that takes into account the column resistance of nanopore walls must be added to explain the testing data.

In the current study, we focus on the experimental investigation on the electric field-induced changes of effective interfacial tension in a nanoporous silica. Compared with other factors that affect the system free energy, such as temperature, using electric field to control wetting or dewetting at a nanopore's inner surface is more straightforward and fast, yet it is still a relatively uninvestigated area.

II. Experimental Section

The concept of contact angle breaks down in a nanopore, since there are only a limited number of liquid molecules in the cross section. Even if an effective contact angle could be defined, e.g., at a Gibbs surface, observing it in the interior of a nanoporous particle is prohibitively difficult. To analyze the solid−liquid interaction in a confining nanoenvironment, a pressure-induced infiltration (PII) experimental setup was designed. The nanoporous phase was produced by using a nanoporous silica provided by Davsil. The as-received material was in particle form, having a large volume fraction of relatively regular nanopores.[40] The particle size was 20−50 μm. In order to increase the degree of hydrophobicity, the inner surfaces of nanopores were modified by silyl groups. About 2 g of the particles were first dehydrated at 100 °C for 36 h, and then immediately immersed in 40 mL 1.5% dry toluene solution of chlorotrimethylsilane. The mixture was refluxed at 90 °C for 20 h. During this process, the hydroxyl groups at nanopore surfaces were deactivated by chlorotrimethylsilane molecules, forming a hydrophobic monolayer,[41] the details of which have been discussed elsewhere.[42,43] The treated silica particles were filtered, washed with dry toluene and warm water, and dried in vacuum at 50 °C for 12 h. The dried silica was placed in a steel mold and compressed by a type 5580 Instron machine at 20 MPa, leading to the formation of nanoporous silica disks. The mass of each disk was 16.5 mg, and the thickness was around 100 μm, with a cross-sectional area of 285 mm^2. Through a gas absorption analysis by using a Micromeritics ASAP-2000 analyzer, it was confirmed that the nanopores were open, as shown in Figure 1. The average nanopore size was 7.4 nm, and the specific nanopore volume was 560 mm^3/g.

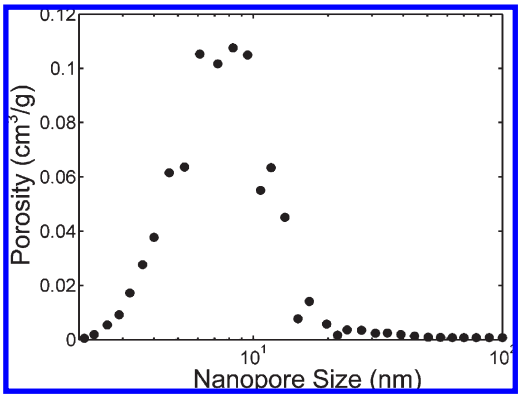

Figure 1. The nanopore volume distribution.

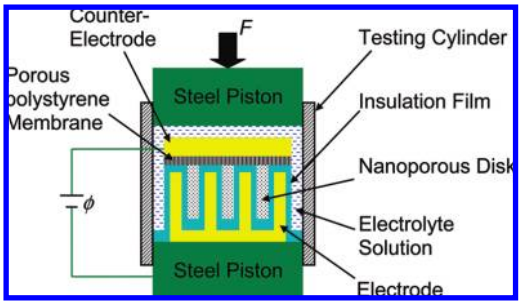

Figure 2. Schematic of the experimental setup. The nanoporous silica disks are about 100 μm thick. They are inserted in between folded aluminum layers coated by 50 μm thick Teflon thin films, and immersed in an electrolyte solution. The counter electrode and the nanoporous silica disks are separated by a 80 μm thick porous membrane separator.

By repeatedly folding an aluminum foil coated with Teflon thin film and inserting the silica disks in between adjacent aluminum layers, a nanoporous layer stack was produced, as depicted in Figure 2. The Teflon film thickness was 50 μm. This structure was condensed in the Instron machine in a steel mold under 0.1 MPa, so that the layers were firmly compressed together. The electrode was placed on a steel piston, with the edges of the aluminum layers in direct contact with the steel. The remaining area of the steel piston was insulated from the liquid phase by a thick layer of epoxy adhesive. The steel piston, together with the layer stack, was placed at the bottom of a steel cylinder, inside which 10 g of 15% potassium chloride (KCl) solution was sealed by another steel piston from the top. The inner surface of the cylinder was insulated from the liquid phase by a Teflon layer. By using a DC power source, an open-circuit voltage, ϕ, was applied between the lower piston and a platinum counter-electrode, which was separated from the silica−aluminum layer stack by a porous polystyrene membrane. The porous membrane thickness was 80 μm, and the pore size was 1−2 μm. The value of ϕ was in the

(26) Punyamurtula, V. K.; Qiao, Y. *Mater. Lett.* **2008**, *62*, 2928–2930.
(27) Kim, T; Han, A; Qiao, Y. *J. Appl. Phys.* **2008**, *104*, 034304.
(28) Han, A; Qiao, Y. *Chem. Eng. J.* **2008**, *141*, 379–382.
(29) Han, A; Punyamurtula, V. K.; Qiao, Y. *Chem. Eng. J.* **2008**, *139*, 426–429.
(30) Kim, T; Lu, W; Han, A; Punyamurtula, V. K.; Chen, X; Qiao, Y. *Appl. Phys. Lett.* **2009**, *94*, 013105.
(31) Han, A; Lu, W; Kim, T; Punyamurtula, V. K.; Qiao, Y. *Smart Mater. Struct.* **2009**, *18*, 024005.
(32) Han, A; Punyamurtula, V. K.; Qiao, Y. *Appl. Phys. Lett.* **2008**, *92*, 153117.
(33) Han, A; Qiao, Y. *J. Mater. Res.* **2007**, *22*, 644–648.
(34) Han, A; Qiao, Y. *Philod. Mag. Lett.* **2007**, *87*, 25–31.
(35) Mattia, D; Gogotsi, Y. *Microfluid. Nanofluid.* **2008**, *5*, 289–305.
(36) Hoeltzel, A; Tallarek, U. *J. Sep. Sci.* **2007**, *30*, 1398–1419.
(37) Han, A; Lu, W; Punyamurtula, V. K.; Chen, X; Surani, F. B.; Kim, T; Qiao, Y. *J. Appl. Phys.* **2008**, *104*, 124908.
(38) Han, A; Lu, W; Kim, T; Chen, X; Qiao, Y. *Phys. Rev. E* **2008**, *78*, 031408.
(39) Qiao, Y; Liu, L; Chen, X. *Nano Lett.* **2009**, *9*, 984–988.
(40) Terasaki, O; Ohsuna, T; Liu, Z; Kaneda, M; Kamiya, S; Carlsson, A; Tsubakiyama, T; Sakamoto, Y; Inagaki, S; Tatsumi, T; Camblor, M. A.; Ryoo, R; Zhao, D; Stucky, G; Shindo, D; Hiraga, K. *Stud. Surf. Sci. Catal.* **2002**, *141*, 27–34.
(41) Han, A; Qiao, Y. *Chem. Lett.* **2007**, *36*, 882–883.
(42) Han, A; Qiao, Y. *Langmuir* **2007**, *23*, 11396–11398.
(43) Lim, M. H.; Stein, A. *Chem. Mater.* **1999**, *11*, 3285.

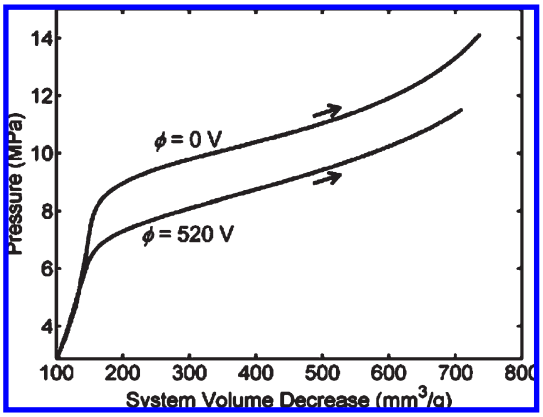

Figure 3. Typical sorption isotherm curves. The system volume decreases as the external pressure is increased. As the PII takes place, an infiltration plateau is formed.

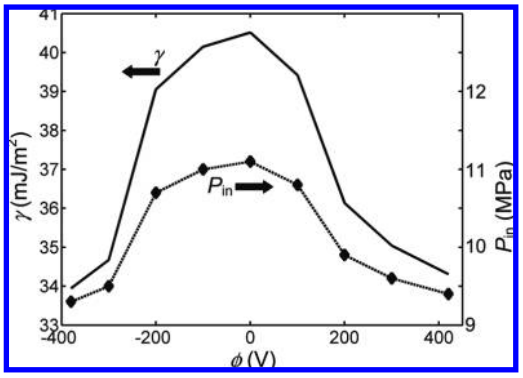

Figure 4. The ion transport pressure (P_{in}) and the effective interfacial tension (γ) as functions of the applied potential difference (ϕ).

range of −380 V to +420 V. By using the Instron machine, the upper piston was intruded into the cylinder at a constant rate of 0.5 mm/min. As the applied load, F, exceeded 4.5 kN, the crosshead was moved back. The quasi-hydrostatic pressure in the liquid phase was calculated as $P = F/A_p$, where $A_p = 286$ mm^2 is the cross-sectional area of the piston. Figure 3 shows typical sorption isotherm curves. The measured ion transport pressure (P_{in}) is given in Figure 4 as a function of the applied voltage. In order to minimize the influence of the definitions of the starting and the ending points of infiltration, the value of P_{in} was taken as the pressure at the middle point of the infiltration plateau, where the slope of the sorption isotherm curve is quite small. Compared with the pressure at the beginning of infiltration, the so-defined P_{in} better reflects the energy exchange between the solid and liquid phases.[39]

A reference test was performed on a large 60 μm thick glass slide, which was surface treated by chlorotrimethylsilane through a process similar to that of the nanoporous silica. A 50 μm thick Teflon layer was firmly compressed with the slide on top of a large aluminum electrode. A drop of 15% potassium chloride solution was placed on the Teflon layer, and its contact angle was measured in situ through a horizontal optical microscope. The external voltage applied between the aluminum electrode and the electrolyte solution was in the same range of −380 V to +420 V. The measurement results are shown in Figure 5.

III. Results and Discussion

At 0 V, the contact angle of the KCl solution at the large glass slide is 121°, indicating that the surface-treated glass is highly hydrophobic. According to the classic Laplace−Young equation, the solid−liquid interfacial tension can be calculated as

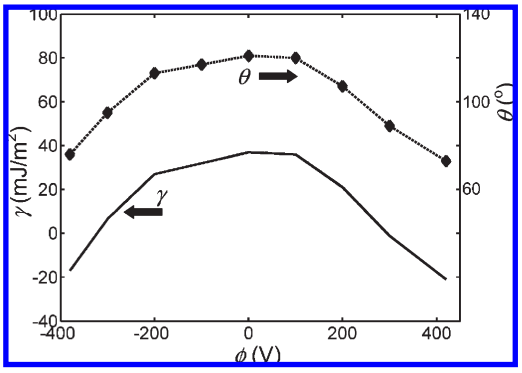

Figure 5. The contact angle (θ) and the interfacial tension (γ) as functions of the applied potential difference (ϕ) at a large flat surface.

$\gamma_{sv} - \gamma_{sl} = \gamma_0 \cdot \cos\theta$,[44] with $\gamma_0 = 74$ mJ/m^2 being the surface tension of the potassium chloride solution. From Figure 5, it can be seen that, when the applied voltage is relatively low, the variation in interfacial tension is mild; as ϕ increases, γ decreases with an increasing rate. The direction of the electric field does not have a pronounced influence on the interfacial tension, and thus the $\phi-\gamma$ curve is quite symmetric. All these phenomena fit well with the prediction of the conventional electrochemistry theory.[45] As the voltage is applied between the electrode and the electrolyte solution, the glass slide and the Teflon layers serve as the insulation phase.

In the setup depicted in Figure 2, the interface of the liquid and solid phases is inside the nanopores. As a result of the silyl treatment, the inner nanopore surfaces are hydrophobic. Therefore, under ambient pressure when the nanoporous silica samples are immersed in the potassium chloride solution, the liquid cannot enter the nanopores, because of the repelling effect of the nanopore walls. When an external pressure is applied by the upper piston, the mechanical work leads to the increase in the system free energy. When the system free energy is sufficiently high, the capillary effect is overcome, and the liquid infiltration starts. Associated with the liquid infiltration, the system volume rapidly decreases with a relatively small pressure increment, and thus a plateau region is formed in the sorption isotherm curve (Figure 3). The liquid transports in the nanopores until the entire nanoporous space is occupied. The width of the infiltration plateau is close to the specific nanopore volume. When the peak pressure is reached and the piston moves out, the pressure in the liquid phases keep decreasing. The unloading behavior of the system is quite different from the loading path, indicating that the system is energy absorbing. The hysteresis may be related to the sliding of liquid molecules and ions along the solid surface,[46,47] the effects of entrapped gas/vapor nanophase,[48,49] and so forth, which is still under investigation and is not the focus of the current study. Note that, while the PII experimental procedure is somewhat similar to mercury porosimetry, the results should not be analyzed by a Washburn type method, since the interfacial tension may not be a constant.

By compressing a unit volume of liquid phase into the nanopores, the work done by the external load is P_{in}. As the nanopore surfaces are in contact with the confined liquid, the system free energy increases by $\gamma \cdot A$, where $A \approx 2/r$ is the specific nanopore

(44) Fay, J. A. *Introduction to Fluid Mechanics*; MIT Press: Cambridge, MA,1994.
(45) Bockris, J. O.; Khan, S. U. M. *Surface Electrochemistry: A Molecular Level Approach*; Plenum Press: New York, 1993.
(46) Chen, X; Cao, G; Han, A; Punyamurtula, V. K.; Liu, L; Culligan, P. J.; Kim, T; Qiao, Y. *Nano Lett*. **2008**, *8*, 2988–2992.
(47) Cao, G; Qiao, Y; Zhou, Q; Chen, X. *Philos. Mag. Lett*. **2008**, *88*, 371–378.
(48) Qiao, Y; Cao, G; Chen, X. *J. Am. Chem. Soc*. **2007**, *129*, 2355–2359.
(49) Han, A; Kong, X; Qiao, Y. *J. Appl. Phys*. **2006**, *100*, 014308.

area per unit nanopore volume, and r is the effective nanopore size. At equilibrium, $\gamma = P_{in} \cdot r/2$; i.e., the system free energy change associated with the liquid infiltration is captured by the effective interfacial tension. According to the gas absorption measurement shown in Figure 1, the media nanopore size is 7.4 nm. The ion/liquid transport pressure corresponding to it, P_{in}, is assessed as the pressure at the intersection of the sorption isotherm curve and the median line between the low-pressure section of loading path and the unloading path. Thus, the values of γ can be calculated as a function of the applied voltage.

When $\phi = 0$, the values of γ of the nanoporous silica and the large glass slide are different. It can be caused by not only the confinement effect of the nanoporus environment, which will be discussed below, but also the different surface coverage due to the distinct surface reaction conditions as well as the differences in the electric loading mode and the thickness and configuration of silica layer. In the current study, we focus on the relative variation of γ associated with the change in external electric field.

It is clear that the measured effective interfacial tension in nanopores decreases as the electric field becomes stronger. The change in γ is quite symmetric with respect to $\phi = 0$. In the setup shown in Figure 2, the dielectric layer between the confined liquid phase and the electrode is the bilayer of Teflon film and silica nanopore wall. While near the Teflon−silica interface the silica layer thickness is quite small, the average silica layer thickness is comparable with that of the large glass slide used in the reference experiment. As the nanopores are filled by the electrolyte solution, the insulation effectiveness of the silica phase is reduced. Hence, if the interface properties in nanopores are similar to that at a large surface, the electrowetting effect on the nanoporous silica should be stronger than the result of the reference experiment.

However, the testing data show that the magnitude of variation of the interfacial tension of the nanoporous sample is much smaller than that in the reference test, even though the average silica layer thickness is thinner. When ϕ is increased from 0 to 420 V, the effective interfacial tension decreases by only about 15%, while, in the reference test in the same voltage range, the interfacial tension changes from positive to negative by more than 140%, nearly 10 times larger. The effective interfacial tension can be regarded as the increase in system free energy per unit area of nanopore inner surface, after the liquid infiltrates into the nanopore. Its dependence on the applied voltage may be attributed to the confinement effect of nanopore walls on the ion transport behavior (Figure 6). At a large surface, outside the outer Helmholtz plane (OHP) there exists a bulk liquid phase, which can be regarded as an infinitely large ion reservoir. When the interface potential becomes different, the electrode-liquid electrostatic energy and the double layer at the insulator-liquid interface would change, both of which lead to the variation in surface ion density; that is, ions tend to move across the OHP into or out of the bulk phase. In the bulk phase, ions are in thermal disarrays. The effective surface ion density can be assessed as the total number of confined ions normalized by the nanopore surface area. In a nanopore, the surface-to-volume ratio is ultrahigh. As a result of the lack of bulk liquid phase in the interior of a nanopore, when the surface potential varies, the motion of ions can quickly make the confined liquid monopolar, creating a reverse double-layer-like structure that prevents the ion structure in the interface layer from being fully developed; that is, the interface capacity tends to be lower compared with that of a large surface. Therefore, while the tendency of interfacial tension variation is the same, its magnitude is reduced.

Another interesting observation is that the $\gamma-\phi$ relation of the nanoporous system cannot be described by the classic equation of $\gamma = \gamma_1 - C\phi^2/2$. Around 200 V, the variation rate of the interfacial tension greatly decreases. In the negative voltage range, there is a similar step. Above the critical voltage, $d\gamma/d\phi$ keeps decreasing as ϕ rises. When ϕ is close to 400 V, the slope of the $\gamma-\phi$ curve is smaller than that at the low-voltage section by about an order of magnitude. The saturation of the electric field effect can also be caused by the small volume-to-surface area ratio of the confined liquid. As the excess ion concentration in the interior is balanced, further increase in potential difference would not cause much variation in the effective ion density in the interface layer, unless ions diffuse away or into the nanopores along the axial direction. In a previous experiment,[50] it was observed that ion exchange between the confined liquid phase and the bulk liquid phase outside the nanoporous particles can be quite slow. The suppression of the ion density change can result in reductions in variations in electrode−liquid electrostatic effect and in silica−liquid interaction, which in turn stabilize the system free energy, so that the effective interfacial tension is less sensitive to the external electric field.

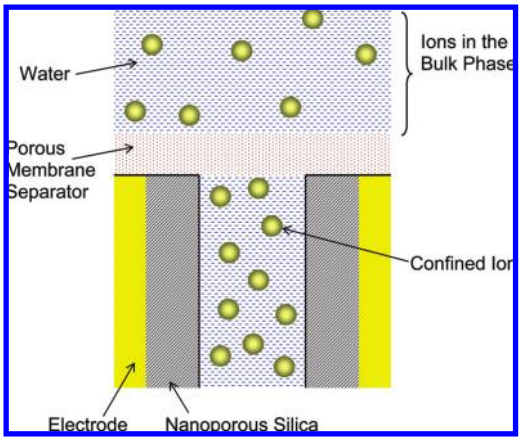

Figure 6. Schematic of confined ions in a nanopore. As a result of the confinement effect of nanopore walls, the effect of external electric field on the effective ion density in nanopores is suppressed.

Note that the above analysis based on the assumption that the lack of bulk liquid phase in nanopores suppresses the electrowetting effect is not directly supported by the experimental evidence. More comprehensive experiments and computer simulations must be performed to eventually validate it, which will be the focus of our future work.

IV. Concluding Remarks

The effective solid−liquid interfacial tension in a nanoporous silica is measured as a function of the applied potential difference. Similar to the prediction of classic electrochemistry theory, the interfacial tension decreases with the increase in potential difference, and the effect of electric field direction is negligible. However, compared with a large solid surface, in the nanopores the electrowetting effect is quite weak, and it tends to be saturated when the voltage is relatively low. One possible cause of these phenomena is the large surface−volume ratio of the confined liquid phase, where the interior cannot be regarded as a neutral, infinitely large ion reservoir.

Acknowledgment. This study was supported by the National Science Foundation and The Sandia National Laboratory under Grant No. CMMI-0705142, and the William J. von Liebig Foundation. Special thanks are also due to Mr. L. A. Operhall for the help with the design of the experimental setup.

(50) Qiao, Y; Punyamurtula, V. K.; Han, A; Lim, H. *J. Power Sources* **2008**, *183*, 403–405.